Laser-induced generation and quenching of magnetization on FeRh studied with time-resolved x-ray magnetic circular dichroism

I. Radu,[1,2,*] C. Stamm,[2] N. Pontius,[2] T. Kachel,[2] P. Ramm,[1] J.-U. Thiele,[3] H. A. Dürr,[2] and C. H. Back[1]
[1]*Department of Physics, Universität Regensburg, 93040 Regensburg, Germany*
[2]*Helmholtz-Zentrum Berlin für Materialien und Energie GmbH, BESSY II, Albert-Einstein-Str. 15, 12489 Berlin, Germany*
[3]*San Jose Research Center, Hitachi Global Storage Technologies, 650 Harry Road, San Jose, California 95120, USA*
(Received 29 July 2009; revised manuscript received 25 January 2010; published 17 March 2010)

Ultrafast magnetization dynamics triggered by femtosecond laser excitation of the FeRh alloy is investigated by time-resolved x-ray magnetic circular dichroism. We measure a gradual growth of magnetization within ≈100 ps for both Fe and Rh elements as the system is laser-driven through its first-order magnetic phase transition from the antiferromagnetic (AFM) to the ferromagnetic (FM) state. A dynamic AFM-FM phase coexistence is observed, identifying the magnetization growth mechanism as the rapid nucleation and subsequent slow expansion of FM regions within an AFM matrix. In contrast to the magnetization generation process, the photoinduced demagnetization of FeRh proceeds on a sub-picosecond time scale. We propose a demagnetization mechanism that follows the electronic temperature of the system developed after laser excitation.

DOI: 10.1103/PhysRevB.81.104415 PACS number(s): 75.40.Gb, 75.30.Kz, 78.70.Dm

In recent years, the feasibility to control and manipulate ferromagnetic order on ultrashort time scales has opened up a vast field of research focused on magnetization dynamics. Most of the experiments have investigated the effect of an ultrashort laser pulse absorbed by the electronic system on the degree of ferromagnetic order. This class of experiments involving various detection techniques has been devoted to the laser-induced *demagnetization* of the 3*d* and 4*f* ferromagnets.[1–7] All these studies converge to the conclusion of a sub-ps demagnetization dynamics. A different class of experiments has investigated the possibility of *generation* of ferromagnetic order in the binary alloy system FeRh. Upon heating, FeRh undergoes an antiferromagnetic to ferromagnetic phase transition at a temperature T_p close to room temperature when the chemically ordered alloy is near the equiatomic composition.[8–11] The antiferromagnetic to the ferromagnetic (AFM-FM) phase transition is accompanied by an isotropic lattice expansion of ≈1%. At higher temperatures the material becomes paramagnetic (PM) around T_c =680 K. Both temperatures are sensitive to the exact composition of the sample and can be tuned by doping.[12]

Recently, two groups independently[13–15] have studied the generation of FM order in the FeRh alloy by means of time-resolved magneto-optical Kerr effect (TR-MOKE). It has been shown, that generating magnetization in FeRh may be considerably faster than the re-establishment of FM order in ordinary ferromagnetic metals when cooling down from the PM state. Cooling is generally limited by heat transfer which occurs typically on nanoseconds time scale. More recently, Bergman *et al.*[15] have used the Landau-Lifshitz-Gilbert formalism to simulate the magnetization growth process as measured in their TR-MOKE data. The authors proposed a model that may explain the development of magnetic order via nucleation and growth of microscopic magnetic domains. Here, we use an alternative approach to probe magnetization dynamics employing time-resolved x-ray magnetic circular dichroism (TR-XMCD). XMCD measures directly the magnetic moment per atom, since it probes the occupation of the valence band in a spin-resolved manner by transitions from well-defined core states.[16]

In this contribution, we employ TR-XMCD on the FeRh alloy to investigate both, the laser-induced AFM-FM phase transition and the transition from the FM toward the PM phase. While we can quench the magnetization on a sub-ps time scale, we observe a rather slow generation of FM order which develops within hundreds of ps. The generation of FM order will be discussed in light of the proposed magnetic domains nucleation model.[15] For the photoinduced demagnetization process we consider a mechanism that follows the transient electronic temperature of the system.

Static and time-resolved XMCD measurements have been performed at the BESSY II UE56/1-PGM beam line that provides soft x-ray light with variable polarization. For the dynamic investigations, we have used the output of an amplified Ti:Sapphire laser as a pump beam and the x-ray synchrotron radiation as a probe. The laser (1 kHz repetition rate, 1.5 eV photon energy, 50 fs pulse length, pulse energy up to 2 mJ) is synchronized at the master clock frequency of the synchrotron. The time resolution of the measurement is ≈50 ps in the normal operation mode of the synchrotron and can be improved to ≈10 ps by employing the so called low-alpha mode.[17] The laser and the x-ray beams are incident on the sample in a nearly collinear configuration under an incidence angle of 30°. The transmitted x-ray intensity is recorded using a boxcar integrator triggered at the repetition rate of the laser. An external magnetic field of 0.5 T is applied along the x-ray beam direction. The dichroic signal is obtained from the difference between the x-ray absorption measured for opposite magnetization orientations at a fixed light helicity. The transient nonmagnetic response of the system is measured employing x-ray absorption spectroscopy (XAS) using linearly polarized light.[6,18,19] For the XMCD measurements, the photon energy is set to the position of maximum absorption, whereas for XAS it is set to the rising slope of the absorption edge (see inset of Fig. 1).

The investigated system is a 30 nm polycrystalline

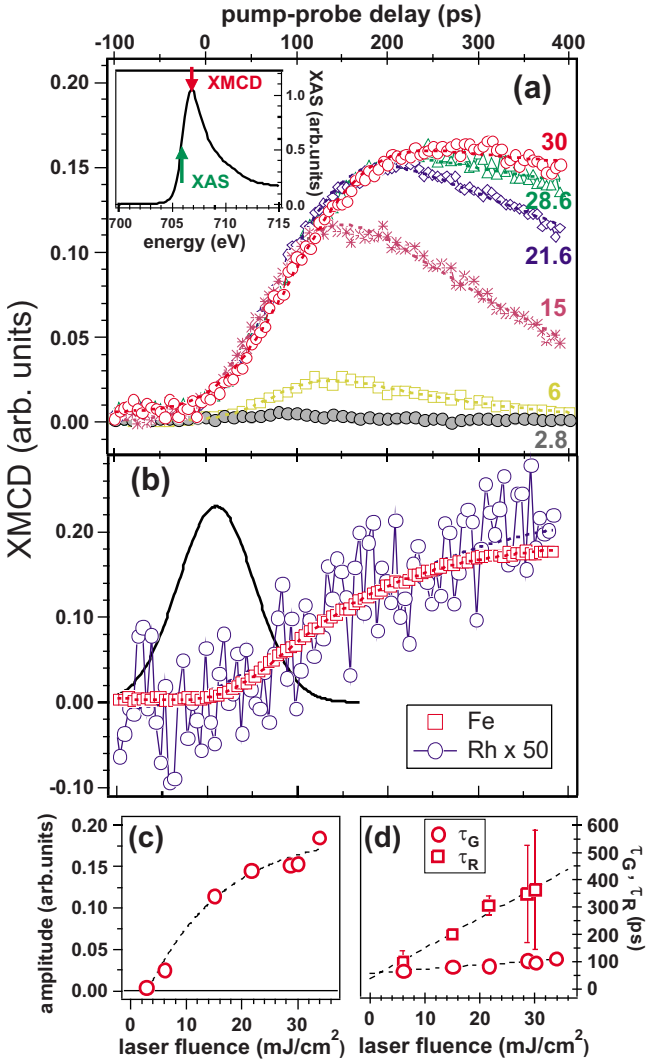

FIG. 1. (Color online) Transient XMCD signal measured at the Fe L_3 and Rh M_3 absorption edges at 100 K. (a) Fe dichroic signal measured as a function of laser fluence in units of mJ/cm^2 as labeled in the figure. The inset depicts the L_3 edge x-ray absorption spectrum of Fe with the arrows indicating the energetic positions where transient XMCD and XAS are measured. (b) Comparison of the Fe and Rh transient dichroism measured at a laser fluence of 33.8 mJ/cm^2. The dashed lines in panels (a) and (b) are fits according to Eq. (1). The amplitude of the magnetization growth component (c) and the time constants for growth and relaxation processes (d) as deduced by fitting the XMCD data with Eq. (1). The time resolution depicted by the Gaussian curve is here ≈50 ps.

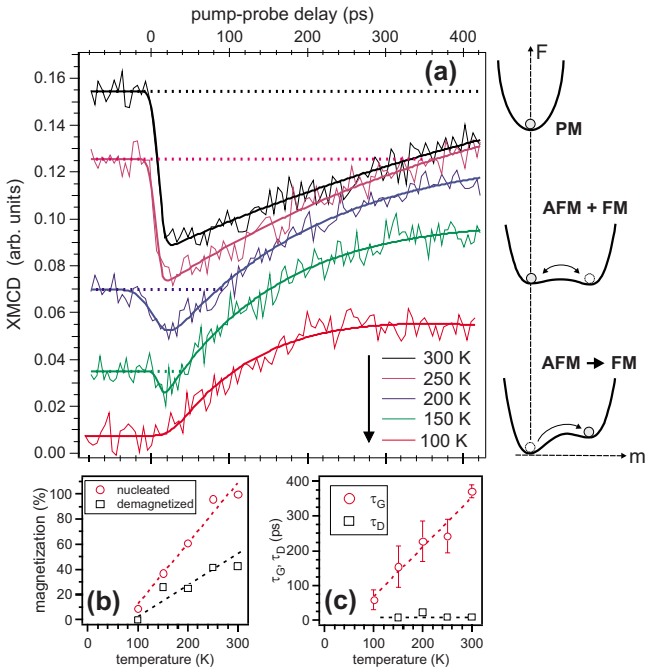

FIG. 2. (Color online) (a) Dichroism measured at Fe L_3 edge with a temporal resolution of ≈10 ps for various temperatures as shown in the figure. The dashed lines indicate the value of the dichroic signal before laser excitation. The thick solid lines are fits according to a biexponential fit function (Refs. 3 and 7). Panel (b) depicts the values of the FM order nucleation and of the reduced magnetization (due to photoinduced demagnetization) deduced from panel (a). Panel (c) shows the variation with temperature of the demagnetization and magnetization growth time constants. On the right-hand side, the schematic diagram of the free energy (**F**) vs magnetic order parameter (**m**) at various temperatures between AFM and FM state.

$Fe_{48.5}Rh_{51.5}$ thin film deposited by magnetron sputtering on a SiN membrane. Addition of ≈1% Ir impurities to FeRh slightly increased the phase transition temperature.[12] The sample is covered with a 200 nm Cu heat sink layer for cooling of the laser excited area. Pt layers of 2.5 nm are used as buffer layers between FeRh and the Cu film and for capping the sample. In the FM state the sample exhibits an in-plane magnetization orientation with a negligible magnetocrystalline anisotropy.

Static, temperature-dependent XMCD measurements of FeRh performed recently by Stamm *et al.*,[11] have shown a constant growth rate for the orbital and spin magnetic moments as the system is thermally driven through the AFM-FM transition. Here, we drive dynamically the AFM-FM phase transition by laser heating the sample. Increasing the laser fluence one should observe a threshold behavior at which the onset of the FM ordering appears and subsequently develops. Such a threshold behavior is considered the signature of the laser-induced phase transition.[14,20,21] The dynamic development of the dichroic signal at the Fe L_3 edge upon increasing the laser fluence is displayed in Fig. 1(a). We observe that a minimum laser fluence between 2.8 and 6 mJ/cm^2 is required to drive the system from the AFM to the FM state at a base temperature of 100 K. Further increasing the fluence, the development of the FM order evolves increasingly slower and eventually saturates for a laser fluence around 30 mJ/cm^2.

In order to extract the time constant of the magnetization growth process and of the subsequent relaxation, we have used the following fit function:

$$f(t) = G*[A(1 - e^{-t/\tau_G}) + Be^{-t/\tau_R}], \quad (1)$$

where the convolution with G represents the time resolution of the experiment (≈50 ps for the data in Fig. 1 and ≈10 ps for the x-ray measurements in Figs. 2–4), A and B are the

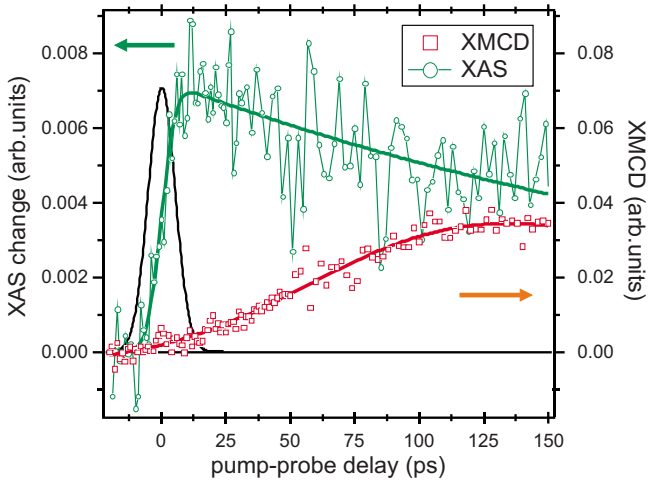

FIG. 3. (Color online) Transient changes in XAS and XMCD measured using linearly and circularly polarized x-ray light, respectively. Both measurements are done at 125 K with 10 ps temporal resolution depicted by the Gaussian profile. The solid lines are fits according to Eq. (1).

exponential amplitudes, and τ_G and τ_R are characteristic time scales for magnetization growth and relaxation, respectively. As seen in Figs. 1(a) and 1(b), the fit function (dashed lines) describes well the experimental data. The retrieved amplitude of the magnetization growth component and the values of τ_G and τ_R are plotted in panels (c) and (d) of Fig. 1, respectively. In the low fluence regime, the amplitude of magnetization generation increases linearly with the laser fluence and saturates at high fluence values. The magnetization growth time constant varies linearly from 67 ± 19 ps to 115 ± 5 ps with increasing fluence from 6 mJ/cm^2 to 33.8 mJ/cm^2 whereas the relaxation time increases with fluence from 100 ± 40 ps to 363 ± 220 ps. The relatively large error bars for the relaxation time—especially for the high fluence regime—arise from the fact that the measured transients do not cover the entire time window of the relaxation process. The relaxation of magnetization back to the AFM state is governed by the heat diffusion out of the laser-excited area, which usually extends to several nanoseconds for metallic samples.

Next, we address the question whether the formation of the magnetic moments at the Fe and Rh sites exhibits any time delay as the system is driven through the phase transition. The comparison of the transient dichroic signal measured at the Fe L_3 edge and Rh M_3 edge is displayed in Fig. 1(b). The curves are measured for an incident laser fluence[22] of 33.8 mJ/cm^2. Despite of the moderate signal to noise ratio due to the reduced absorption cross section at the Rh M edges, we observe that both elements show a similar growth of FM order vs pump-probe delay. Using Eq. (1) we obtain τ_G time constants of 115 ± 5 ps and 160 ± 47 ps for Fe and Rh, respectively. Based on these results we can conclude that, within experimental accuracy, the ferromagnetic ordering at the Fe and Rh sites develops in a similar manner with a time constant of ≈ 120 ps at this particular laser fluence.

In order to get a deeper understanding of the magnetization growth mechanism we have measured the transient dichroic response of FeRh at intermediate temperatures between the AFM and FM phase (100 to 300 K). Figure 2(a) shows the transient dichroic signal measured at the Fe L_3 edge with a temporal resolution of 10 ps and a laser fluence of 12 mJ/cm^2. At 100 K, we observe the typical behavior of magnetization growth (see Fig. 1) with a slow rise time within hundreds of ps. For intermediate temperatures (150 to 250 K) we notice an initial sudden drop of dichroism followed by a rapid recovery (its level is indicated by the dashed lines in Fig. 2) superimposed on the slow magnetization rise behavior. Clearly, for this temperature range, two competing processes are present: (i) a rapid demagnetization of the already nucleated FM regions within the first 10 ps followed by remagnetization and (ii) the slow magnetization growth arising from the AFM matrix that incorporates the FM domains. In the high temperature phase (300 K), the demagnetization process becomes dominant being accompanied by the diminishing and eventual disappearance of the magnetization growth component.

The existence of two opposite processes-demagnetization of FM ordered areas and the magnetization generation arising from AFM state-within the same pump-probe transient gives evidence for an AFM-FM phase coexistence in a strongly nonequilibrium regime. Such a dynamic AFM-FM phase coexistence can be qualitatively understood within the schematic diagram of the free energy potential (**F**) vs magnetic order parameter (**m**) plotted on the right-hand side of Fig. 2. For clarity, we also show in Fig. 2(b) the relative contributions of the magnetization nucleation and demagnetization processes to the transient XMCD signal.[23] At low temperatures the system is driven from the ground AFM state to the excited FM state upon fs laser irradiation, with an initial FM nucleation of $\approx 9\%$ and no presence of demagnetization. At intermediate temperatures, the energy barrier between AFM and FM states is reduced which leads to a coexistence of both phases.[24] This is reflected in the FM nucleation values, which increase significantly from 9% at 100 K to 37% at 150 K and up to 96% at 250 K, and simultaneously in the appearance of demagnetization ranging from 25% to 42% across this temperature interval. At 300 K and in the presence of the laser excitation, the AFM-FM transition is completed, which means 100% magnetization nucleation with the sample being in a single FM domain state. For this temperature the sample is partially demagnetized (to about 45%) and eventually promoted to the PM state by further increasing the temperature [see Fig. 4(b)] or the laser fluence (not shown). Due to their different characteristic time scales, the rapid demagnetization of the FM regions and the slow magnetization generation process evolve on distinct time intervals in the transient data. By fitting the data with a biexponential fit function,[3,7] the characteristic time scales of the demagnetization (τ_D) and magnetization growth (τ_G) processes are deduced.[25] The results are shown in Fig. 2(c). While the time constant of magnetization growth increases from 60 ps to 370 ps the demagnetization time τ_D remains essentially constant around 10 ps (limited by time resolution) for all temperatures.

We emphasize that these results demonstrate the phase coexistence of the AFM and FM states in a highly nonequilibrium regime during the fs laser-induced AFM-FM phase

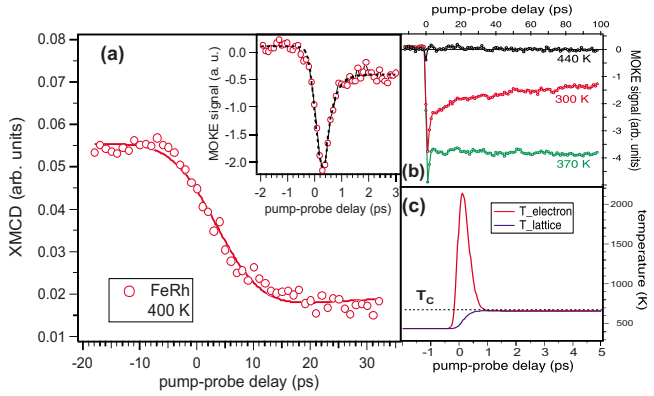

FIG. 4. (Color online) (a) Laser-induced demagnetization of FeRh measured at the L_3 edge of Fe at 400 K. The solid line is a fit described by the convolution of step function with a Gaussian of 10 ps width. The inset depicts the transient demagnetization dynamics measured on the same FeRh sample using TR-MOKE with fs time resolution. The dashed line is a fit described by a biexponential function (Ref. 3 and 7). (b) TR-MOKE data measured on FeRh at various temperatures. (c) Two-temperature model simulation done for a sample temperature of 440 K.

transition. This is a prerequisite for a magnetization growth mechanism based on the initial nucleation of the FM state within an AFM matrix. Although such a magnetization growth scenario has been postulated by Bergman *et al.*,[15] no direct observation has been reported yet. As to the peculiar observation of a sub-ps magnetization onset ($\approx$15% of the magnetization final value) reported in earlier TR-MOKE measurements,[14] our data do not exhibit this feature, being most likely smeared-out at the employed time resolution of 10 ps.

To investigate the electronic contribution to the AFM-FM transition we employ *linearly polarized* x-rays, which probe the laser-induced *nonmagnetic* response[6,18,19] of the system. Figure 3 depicts the transient changes in XAS and, for comparison, the dynamic XMCD response. Both transients are measured at a temperature of 125 K and 10 mJ/cm^2 laser fluence. We observe a rapid increase of the transient absorption that reaches its maximum within 10 ps after excitation (i.e., the time resolution) while only small XMCD changes (at 10 ps it reaches $\approx$5% of the maximum XMCD value) are present. In the following 100 ps, we observe the slow relaxation of the XAS response accompanied by the onset and the slow rise of the magnetic signal. The clearly distinct time scales of the magnetization growth (here 82 ± 6 ps) and of the transient optical response ($\leq$10 ps) show that the electron and lattice dynamics (measured here by transient XAS) are driving the FM order development. To what extent the lattice or the electronic system are involved in driving the phase transition remains a subject for further studies with sub-ps time resolution. However, a ps time scale evolution of the electron and lattice dynamics supports the model of Bergman *et al.*[15] regarding the time range for the initial generation of local magnetization.

At this stage we return to the laser-induced demagnetization of FeRh. For this purpose we heat FeRh to the FM phase, e.g., at 400 K, and monitor the fs laser-induced demagnetization dynamics by measuring the dichroic signal at the Fe L_3 edge. A typical demagnetization transient measured on the FeRh sample with $\approx$10 ps time resolution and a laser fluence of 20 mJ/cm^2 is displayed in Fig. 4(a). We observe a reduction of the dichroic signal by 72% that takes place within 15 ps after photo-excitation. This time scale represents only an upper limit for the demagnetization process at the employed time resolution. For an unambiguous determination of the demagnetization time scale we employ time-resolved magneto-optics with 170 fs time resolution (see Ref. 26 for experimental details) on the very same sample under comparable experimental conditions. The measured demagnetization dynamics, shown in the inset of Fig. 4(a), takes place within 400 fs after laser excitation. Using a biexponential fit function[3,7] we retrieve a characteristic demagnetization time scale of 200 ± 20 fs. As shown in Fig. 4(b), increasing further the temperature (e.g., to 440 K) we promote the system into the PM state within the laser pulse duration. Simulations according to the two-temperature model[27] done for FeRh at 440 K [see Fig. 4(c)] reveal a maximum electronic temperature of 2000 K that overcomes the Curie temperature T_c=680 K within the first 100 fs after laser excitation. Accounting for the observed demagnetization time scale and for the simulated transient electronic energy flow we propose a demagnetization mechanism that follows the electronic temperature of the system.

Summarizing, we have used time-resolved x-ray spectroscopy to investigate the laser-induced first-order AFM-FM magnetic phase transition as well as the FM-PM transition on FeRh thin films. Upon fs laser excitation, the generation of ferromagnetic order occurs within hundreds of ps for both Fe and Rh magnetic moments. Transient XMCD data measured at temperatures between the AFM and FM states reveal an AFM-FM phase coexistence in a nonequilibrium regime, which provides the required conditions for a magnetization growth mechanism based on FM domain nucleation within an AFM matrix. Simultaneously, the transient nonmagnetic response of the system, including the lattice expansion triggered by the AFM-FM transition, evolves on a ps time scale being mainly limited by the experimental temporal resolution of 10 ps. Although this observation suggests a lattice-driven magnetic phase transition, future time-resolved XMCD measurements with fs time resolution[6] are needed to settle the dilemma of a lattice- or magnetization-driven AFM-FM phase transition in FeRh. On the other hand, the photoinduced demagnetization of FeRh proceeds considerably faster, complementary TR-MOKE studies revealing a characteristic time constant of $\approx$200 fs when the excitation energy resides in the electronic system.

Financial support by the Deutsche Forschungsgemeinschaft through the Priority Programme 1133 "Ultrafast Magnetization Processes" is gratefully acknowledged.

*Present address: Institute for Molecules and Materials, Radboud University Nijmegen, 6525 AJ Nijmegen, The Netherlands; i.radu@science.ru.nl

[1] E. Beaurepaire, J.-C. Merle, A. Daunois, and J.-Y. Bigot, Phys. Rev. Lett. **76**, 4250 (1996).
[2] J. Hohlfeld, E. Matthias, R. Knorren, and K. H. Bennemann, Phys. Rev. Lett. **78**, 4861 (1997).
[3] L. Guidoni, E. Beaurepaire, and J. Y. Bigot, Phys. Rev. Lett. **89**, 017401 (2002).
[4] M. Lisowski, P. A. Loukakos, A. Melnikov, I. Radu, L. Ungureanu, M. Wolf, and U. Bovensiepen, Phys. Rev. Lett. **95**, 137402 (2005).
[5] B. Koopmans, Spin Dynamics in Confined Magnetic Structures II, Top. Appl. Phys. Vol. 87, (Springer, New York, 2003).
[6] C. Stamm, T. Kachel, N. Pontius, R. Mitzner, T. Quast, K. Holldack, S. Khan, C. Lupulescu, E. F. Aziz, M. Wietstruk, H. A. Dürr, and W. Eberhardt, Nature Mater. **6**, 740 (2007).
[7] I. Radu, G. Woltersdorf, M. Kiessling, A. Melnikov, U. Bovensiepen, J.-U. Thiele, and C. H. Back, Phys. Rev. Lett. **102**, 117201 (2009).
[8] M. Fallot and R. Hocart, Rev. Sci. **77**, 498 (1939).
[9] J. S. Kouvel and C. C. Hartelius, J. Appl. Phys. **33**, 1343 (1962).
[10] S. Maat, J. U. Thiele, and E. E. Fullerton, Phys. Rev. B **72**, 214432 (2005).
[11] C. Stamm, J.-U. Thiele, T. Kachel, I. Radu, P. Ramm, M. Kosuth, J. Minár, H. Ebert, H. A. Dürr, W. Eberhardt, and C. H. Back, Phys. Rev. B **77**, 184401 (2008).
[12] J. U. Thiele, S. Maat, J. L. Robertson, and E. E. Fullerton, IEEE Trans. Magn. **40**, 2537 (2004).
[13] J. U. Thiele, M. Buess, and C. H. Back, Appl. Phys. Lett. **85**, 2857 (2004).
[14] G. Ju, J. Hohlfeld, B. Bergman, R. J. M. van de Veerdonk, O. N. Mryasov, J.-Y. Kim, X. Wu, D. Weller, and B. Koopmans, Phys. Rev. Lett. **93**, 197403 (2004).
[15] B. Bergman, G. Ju, J. Hohlfeld, R. J. M. van de Veerdonk, J.-Y. Kim, X. Wu, D. Weller, and B. Koopmans, Phys. Rev. B **73**, 060407(R) (2006).
[16] P. Carra, B. T. Thole, M. Altarelli, and X. Wang, Phys. Rev. Lett. **70**, 694 (1993).
[17] M. Abo-Bakr, J. Feikes, K. Holldack, G. Wüstefeld, and H. W. Hubers, Phys. Rev. Lett. **88**, 254801 (2002).
[18] T. Kachel, N. Pontius, C. Stamm, M. Wietstruk, E. F. Aziz, H. A. Dürr, W. Eberhardt, and F. M. F. de Groot, Phys. Rev. B **80**, 092404 (2009).
[19] A. Cavalleri, M. Rini, H. H. W. Chong, S. Fourmaux, T. E. Glover, P. A. Heimann, J. C. Kieffer, and R. W. Schoenlein, Phys. Rev. Lett. **95**, 067405 (2005).
[20] N. Gedik, D.-S. Yang, G. Logvenov, I. Bozovic, and A. H. Zewail, Science **316**, 425 (2007).
[21] M. Rini, Z. Hao, R. W. Schoenlein, C. Giannetti, F. Parmigiani, S. Fourmaux, J. C. Kieffer, A. Fujimori, M. Onoda, S. Wall, and A. Cavalleri, Appl. Phys. Lett. **92**, 181904 (2008).
[22] The reflectivity of FeRh at 800 nm is about 75%, which gives a lower value for the actual absorbed laser fluence.
[23] The magnetization nucleation value is defined as the ratio between the XMCD signal measured at negative delays and the final XMCD value while the demagnetization value is defined as the ratio between the level of the rapid drop of the XMCD signal and the signal measured at negative delays.
[24] XMCD measurement averages over the nucleated FM areas within a 1 mm probing x-ray spot. The size of these nucleated areas varies form 0.3 to 3 micrometers as deduced from static PEEM measurements.
[25] We note that in the temperature range of the AFM-FM phase coexistence τ_G measures a combination of magnetization growth and remagnetization (following the demagnetization) processes.
[26] M. Binder, A. Weber, O. Mosendz, G. Woltersdorf, M. Izquierdo, I. Neudecker, J. R. Dahn, T. D. Hatchard, J.-U. Thiele, C. H. Back, and M. R. Scheinfein, Phys. Rev. B **74**, 134404 (2006).
[27] S. I. Anisimov, B. L. Kapeliovich, and T. L. Perel'man, Sov. Phys. JETP **39**, 375 (1974).